

## UC Davis

### UC Davis Previously Published Works

**Title**

Isolation and Crystallographic Characterization of Gd<sub>3</sub>N@D 2(35)-C88 through Non-Chromatographic Methods

**Permalink**

<https://escholarship.org/uc/item/7f8008m3>

**Journal**

Inorganic Chemistry, 55(1)

**ISSN**

0020-1669

**Authors**

Stevenson, Steven  
Arvola, Kristine D  
Fahim, Muska  
et al.

**Publication Date**

2016-01-04

**DOI**

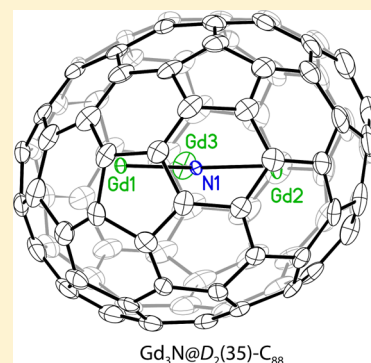
10.1021/acs.inorgchem.5b01814

Peer reviewed

Isolation and Crystallographic Characterization of  $\text{Gd}_3\text{N}@D_2(35)\text{-C}_{88}$  through Non-Chromatographic MethodsSteven Stevenson,<sup>\*,†</sup> Kristine D. Arvola,<sup>†</sup> Muska Fahim,<sup>†</sup> Benjamin R. Martin,<sup>†</sup> Kamran B. Ghiassi,<sup>‡</sup> Marilyn M. Olmstead,<sup>\*,‡</sup> and Alan L. Balch<sup>\*,‡</sup><sup>†</sup>Department of Chemistry, Indiana-Purdue University Fort Wayne (IPFW), 2101 E. Coliseum Blvd, Fort Wayne, Indiana 46805, United States<sup>‡</sup>Department of Chemistry, University of California, Davis, One Shields Avenue, Davis, California 95616, United States

## S Supporting Information

**ABSTRACT:** While several nonchromatographic methods are available for the isolation and purification of endohedral fullerenes of the type  $\text{M}_3\text{N}@I_h\text{-C}_{80}$ , little work has been done that would allow other members of the  $\text{M}_3\text{N}@C_{2n}$  family to be isolated with minimal chromatography. Here, we report that  $\text{Gd}_3\text{N}@D_2(35)\text{-C}_{88}$  can be isolated from the multitude of endohedral and empty cage fullerenes present in carbon soot obtained by electric-arc synthesis using  $\text{Gd}_2\text{O}_3$ -doped graphite rods. The procedure developed utilizes successive precipitation with the Lewis acids  $\text{CaCl}_2$  and  $\text{ZnCl}_2$  followed by treatment with amino-functionalized silica gel. The structure of the product was identified by single-crystal X-ray diffraction.



## INTRODUCTION

Since the discovery of  $\text{Sc}_3\text{N}@I_h\text{-C}_{80}$ , the third most readily prepared fullerene after  $\text{C}_{60}$  and  $\text{C}_{70}$ ,<sup>1</sup> considerable attention has been given to the preparation, isolation, and purification of various members of the  $\text{M}_3\text{N}@I_h\text{-C}_{80}$  family. The chemical reactivities of this family of endohedrals have also been extensively studied.<sup>2</sup> Generally, purification of  $\text{Sc}_3\text{N}@I_h\text{-C}_{80}$  and other endohedral fullerenes relies on high-performance liquid chromatography (HPLC), frequently involving multiple columns and a variety of solvents.<sup>3,4</sup> Alternatively, several non-chromatographic methods have been developed to enrich or chemically purify members of the  $\text{M}_3\text{N}@I_h\text{-C}_{80}$  family, including mixed-metal cases where the  $\text{M}_3\text{N}$  unit contains two or even three different metals.<sup>5–15</sup> Chemical means of purification of the  $\text{M}_3\text{N}@I_h\text{-C}_{80}$  family frequently relies upon the observation that these molecules are less reactive toward addition reactions than other endohedral fullerenes or empty cage fullerenes.

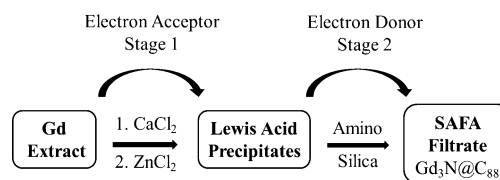
In addition to the  $\text{M}_3\text{N}@I_h\text{-C}_{80}$  family of endohedral fullerenes, related molecules with larger or smaller cage sizes have been identified and purified by standard HPLC techniques. For example, the individual members of the  $\text{Gd}_3\text{N}@C_{2n}$  ( $2n = 78$  to  $88$ ) family have been isolated and, except for  $\text{Gd}_3\text{N}@C_{88}$ , crystallographically characterized.<sup>16–18</sup> These gadolinium-containing molecules have potential medical applications as magnetic resonance imaging agents.<sup>19–22</sup> However, alternative, non-HPLC means of purification and isolation of the  $\text{Gd}_3\text{N}@C_{2n}$  family have not been explored. Moreover, the lack of means to obtain these endohedrals

readily has meant that their chemical reactivity is unexplored. Here, we present a useful, non-chromatographic method to obtain the largest member of the  $\text{Gd}_3\text{N}@C_{2n}$  family in pure form and to determine its structure by single-crystal X-ray diffraction.

## RESULTS AND DISCUSSION

**Isolation of  $\text{Gd}_3\text{N}@C_{88}$  from Carbon Soot.** An overview of our non-HPLC approach to the isolation of  $\text{Gd}_3\text{N}@C_{88}$  is shown in Scheme 1. Stage 1 utilizes selective fractionation of Gd endohedrals by successive precipitation with two Lewis acids, namely,  $\text{CaCl}_2$  and  $\text{ZnCl}_2$ .<sup>10,15,23,24</sup> Stage 2 provides further selectivity by manipulating chemical reactivity differences of the various fullerenes and endohedral fullerenes with nucleophilic amines immobilized onto a solid support (stir and

**Scheme 1. Overview of Purifying  $\text{Gd}_3\text{N}@C_{88}$  by Selective Reactions with Lewis Acids (Stage 1) and Aminosilica (Stage 2)**



Received: August 8, 2015

Published: September 30, 2015

filter approach or SAFA).<sup>9,11,12,25</sup> By combining the selectivity of two different types of reagents (i.e., electron-poor and electron-rich),  $\text{Gd}_3\text{N}@C_{88}$  can now be isolated using simple solution chemistry, as opposed to the conventional method of HPLC as the sole separation method. The existence of  $\text{Gd}_3\text{N}@C_{88}$  has been noted for many years;<sup>16–18</sup> yet the X-ray crystal structure remained unsolved until now, due in part to its low abundance and difficulty in removing traces of fullerene and metallofullerene contaminants. As the data in Table 1 show,

**Table 1. First Oxidation Potentials for the  $\text{Gd}_3\text{N}@C_{2n}$  Family**

endohedral	first oxidation potential (V) <sup>a</sup>	reference
$\text{Gd}_3\text{N}@C_{88}$	+0.06	ref 16
$\text{Gd}_3\text{N}@C_{84}$	+0.32	ref 16
$\text{Gd}_3\text{N}@C_{86}$	+0.35	ref 24
$\text{Gd}_3\text{N}@C_{82}$	+0.37	ref 24
$\text{Gd}_3\text{N}@C_{80}$	+0.58	ref 16

<sup>a</sup>In *o*-dichlorobenzene solution with 0.05 M (*n*-Bu<sub>4</sub>N)(PF<sub>6</sub>) as supporting electrolyte with ferrocene/ferrocinium reference.

$\text{Gd}_3\text{N}@C_{88}$  has a remarkably low first oxidation potential.<sup>16,26</sup> Since a correlation between the first oxidation potential for endohedral fullerenes and the strength of the Lewis acid needed for precipitation has been observed, the low oxidation potential of  $\text{Gd}_3\text{N}@C_{88}$  should allow it to preferentially precipitate with weak Lewis acids.

Graphite rods containing  $\text{Gd}_2\text{O}_3$  and copper metal were vaporized in an electric-arc generator under a helium/dinitrogen atmosphere to produce fullerene-containing soot as described previously.<sup>27</sup> This soot was extracted with xylenes to produce a soluble extract. The laser desorption ionization (LDI) spectrum of this soluble Gd soot extract is shown in Figure 1a. The extract contains a variety of empty cage fullerenes and various gadolinium-containing endohedral fullerenes.

A 1.5 g portion of this extract was dissolved in 1 L of carbon disulfide and subsequently subjected to four rounds of treatment with solid Lewis acids. In Round 1, 1.2 g of solid  $\text{CaCl}_2$  was added. After it was stirred for 3.75 h, the mixture was filtered, and the filtrate was saved for Round 2 of treatment. The precipitate from Round 1 was then transferred to a beaker containing ice, water, and carbon disulfide for recovery of the endohedrals from the precipitate. After multiple washes with water in a separatory funnel, the decomplexed metallofullerenes were recovered from the bottom layer of carbon disulfide. Figure 1b shows that this sample is enriched in  $\text{Gd}@C_{82}$  and contains few of the empty cage fullerenes.

In Round 2, 3.4 g of anhydrous, solid  $\text{CaCl}_2$  was added, and the suspension was stirred for 7.75 d. The solid was again removed by filtration, and the filtrate was saved for Round 3. The solid material was treated with ice, water, and carbon disulfide to recover the endohedrals in the carbon disulfide layer. Mass spectral analysis as seen in Figure 1c shows that this sample contains a variety of endohedrals including  $\text{Gd}@C_{82}$  and many members of the  $\text{Gd}_2C_{2n}$  family.

For Round 3, 2.0 g of anhydrous  $\text{ZnCl}_2$  powder was added to the filtrate from Round 2, and the mixture was stirred for 4 h. Subsequently, the solid was collected by filtration and treated with ice, water, and carbon disulfide as described above. The mass spectrum shown in Figure 1d reveals that some  $\text{Gd}@C_{82}$  is still present but that  $\text{Gd}_3\text{N}@C_{92}$  and  $\text{Gd}_3C_{102}$  are prominent,

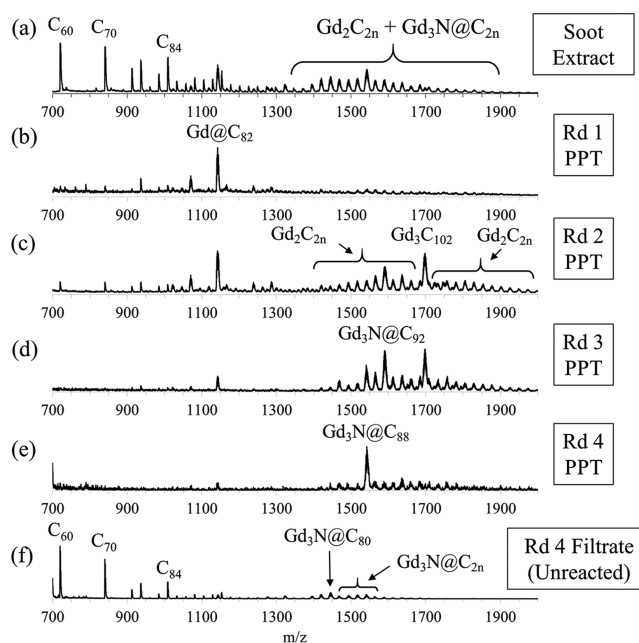


**Figure 1.** LDI spectra of (a) soluble Gd soot extract, (b, c) endohedrals selectively isolated from Rounds 1 and 2 of precipitation with  $\text{CaCl}_2$ , (d, e) Rounds 3–4 of precipitation with  $\text{ZnCl}_2$ , and (f) unreactive fullerenes and endohedrals in the filtrate from Round 4.

along with members of the  $\text{Gd}_3\text{N}@C_{2n}$  and  $\text{Gd}_2C_{2n}$  families.  $\text{Gd}_3C_{102}$  and other  $\text{M}_3C_{102}$  ( $\text{M} = \text{Lu}, \text{Dy}, \text{Tb}$ ) compounds have recently been discovered and shown to be remarkably stable.<sup>28</sup>

In the final round, Round 4, the filtrate from Round 3 was treated with 2.1 g of anhydrous  $\text{ZnCl}_2$  powder and allowed to stir for 7 d. The solids were collected by filtration and treated with the usual ice, water, and carbon disulfide mixture. Mass spectral analysis of the carbon disulfide layer reveals the presence of the target  $\text{Gd}_3\text{N}@C_{88}$  as the dominant material in the recovered sample as seen in Figure 1e. Figure 1f shows the mass spectrum of the contents of the filtrate from the final round of Lewis acid treatment. Empty cage fullerenes and other members of the  $\text{Gd}_3\text{N}@C_{2n}$  family have survived the Lewis acid treatments. The enrichment of  $\text{Gd}_3\text{N}@C_{88}$  from the initial soot extract as shown in Figure 1a to the Round 4 precipitate (Figure 1e) is remarkable, given the complexity of the initial sample.

Because the Lewis acid approach still revealed low-level amounts of  $\text{Gd}_2C_{2n}$  contaminants in the Round 4 precipitate, a different type of chemical reaction was implemented to achieve further purification. On the basis of prior reports of the use of aminosilica for endohedral separations,<sup>9,11,12,25</sup> we investigated the feasibility of further purification of  $\text{Gd}_3\text{N}@C_{88}$  with the stir and filter approach using aminosilica.

A 5 mg sample of enriched  $\text{Gd}_3\text{N}@C_{88}$  from the Round 4 precipitate was dissolved in 90 mL of xylenes and stirred with fresh, vacuum-dried aminosilica for 22 h. The progress was followed as shown in Figure 2. An isolated sample of 3 mg of  $\text{Gd}_3\text{N}@C_{88}$  (~90% purity) was obtained from the filtrate as seen in Figure 2c, where it is compared to the original soot extract in Trace (a) and the product of the Lewis acid treatment in Trace (b). Note that the  $\text{Gd}_2C_{2n}$  contaminants were immobilized onto the aminosilica. To provide the X-ray crystallographic experiment with maximal purity, a single HPLC pass was performed on a BuckyPrep-M column. The chromatogram of this final purified sample is shown in Figure

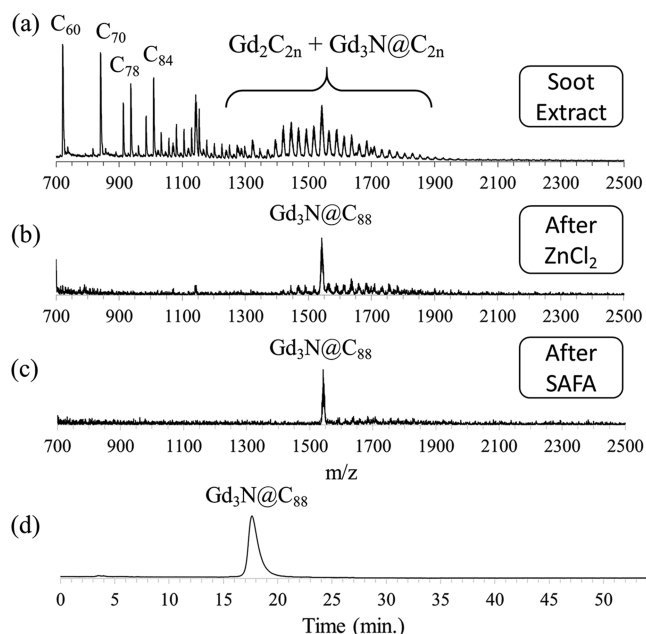


**Figure 2.** LDI mass spectra showing the progression of chemical isolation of  $\text{Gd}_3\text{N}@C_{88}$  from (a) Gd soot extract, (b) precipitation and recovery from  $\text{ZnCl}_2$ , (c) further purification using aminosilica in a SAFA step, and (d) chromatogram for the X-ray purity sample, BuckyPrep-M column, 1 mL/min xylenes, 360 nm UV detection, and 400  $\mu\text{L}$  injection.

2d. The LDI mass spectrum obtained from this  $\text{Gd}_3\text{N}@C_{88}$  sample is provided in the [Supporting Information](#).

**Crystallographic Characterization of  $\text{Gd}_3\text{N}@D_2(35)\text{-C}_{88}$ .** For the X-ray diffraction study, a toluene solution of  $\text{Gd}_3\text{N}@D_2(35)\text{-C}_{88}$  in toluene was layered over a saturated solution of  $\text{Ni}(\text{OEP})$  (OEP is the dianion of octaethylporphyrin) in toluene to produce black blocks of  $\text{Gd}_3\text{N}@D_2(35)\text{-C}_{88}\cdot\text{Ni}(\text{OEP})\cdot 2(\text{toluene})$ . The crystallographic results show that the  $D_2(35)\text{-C}_{88}$  cage is present in these crystals, but two orientations of the chiral cage occupy a common site. A drawing of one enantiomer of  $\text{Gd}_3\text{N}@D_2(35)\text{-C}_{88}$  is shown in [Figure 3](#). The  $D_2(35)\text{-C}_{88}$  cage has a somewhat squashed shape. Thus, the distances across the cage along the three  $C_2$  axes reveal one short span, 7.254 Å, and two longer distances, 8.530 and 8.829 Å.

The  $\text{Gd}_3\text{N}$  group inside the cage shows disorder, but there is only one position for the nitride ion. Three orientations of the interior  $\text{Gd}_3$  unit are clearly evident and were refined with the following occupancies (Gd1, Gd2, Gd3: 0.2314(7); Gd4, Gd5, Gd6: 0.1525(9); Gd7, Gd8, Gd9: 0.0802(8)). There also are three additional Gd positions (Gd10, Gd11, Gd12) that did not form a defined cluster and probably share other Gd positions. [Figure 3](#) shows the position of the major  $\text{Gd}_3\text{N}$  unit and the close contacts made between those gadolinium ions and the cage carbon atoms. For the major  $\text{Gd}_3\text{N}$  orientation, the Gd–N distances are 2.1402(17) Å for Gd1, 2.216(3) Å for Gd2, and 2.181(3) Å for Gd3. A selection of other Gd–N and Gd–C distances is given in [Table 2](#). The three major  $\text{Gd}_3\text{N}$  groups are planar. The sum of the three Gd–N–Gd angles for these clusters are Gd1, Gd2, Gd3: 359.9°; Gd4, Gd5, Gd6: 360.0°; Gd7, Gd8, Gd9: 360.0°.

Overall, our results show that the structure of  $\text{Gd}_3\text{N}@D_2(35)\text{-C}_{88}$  is similar to those of  $\text{Tb}_3\text{N}@D_2(35)\text{-C}_{88}$ <sup>29</sup> and  $\text{Tm}_3\text{N}@D_2(35)\text{-C}_{88}$ ,<sup>30</sup> whose structures have been determined

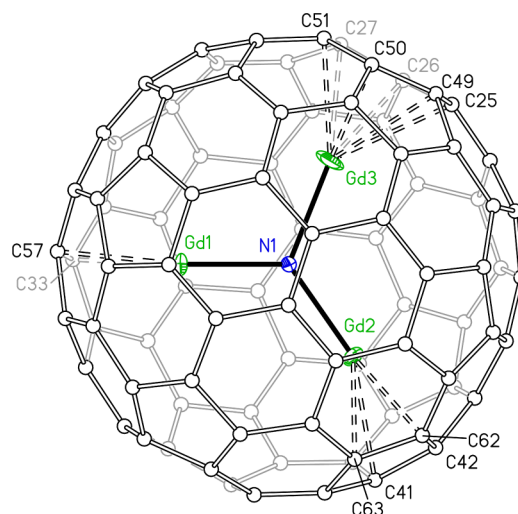


**Figure 3.** A drawing of one enantiomer of  $\text{Gd}_3\text{N}@D_2(35)\text{-C}_{88}$  in  $\text{Gd}_3\text{N}@D_2(35)\text{-C}_{88}\cdot\text{Ni}(\text{OEP})\cdot 2(\text{toluene})$  with the major orientation of the  $\text{Gd}_3\text{N}$  group. The short, two-fold axis of the cage is nearly perpendicular to the plane of the figure and passes through N1. The closest contacts between the carbon atoms of the  $\text{C}_{88}$  cage and the Gd ions are indicated by the dashed lines.

**Table 2. Selected Interatomic Distances (Å) in  $\text{Gd}_3\text{N}@D_2(35)\text{-C}_{88}$**

	Gd1	Gd2	Gd3		
N1	2.1402(17)	N1	2.216(3)	N1	2.181(3)
C33	2.3655(15)	C41	2.5614(16)	C25	2.642(3)
C57	2.4516(16)	C42	2.4057(14)	C26	2.502(3)
		C62	2.3746(13)	C27	2.407(3)
		C63	2.5022(15)	C49	2.624(3)
				C50	2.522(2)
				C51	2.443(2)
	Gd4	Gd5	Gd6		
N1	2.234(3)	N1	2.131(3)	N1	2.2559(17)
	Gd7	Gd8	Gd9		
N1	2.167(5)	N1	2.142(3)	N1	2.149(6)

by single-crystal X-ray diffraction. The  $D_2(35)\text{-C}_{88}$  cage in all three of these compounds shows a similar degree of flattening. The distances along the three twofold axes in these molecules follow a similar pattern with one short and two longer distances as follows:  $\text{Gd}_3\text{N}@D_2(35)\text{-C}_{88}$ , 7.254, 8.530, 8.829 Å;  $\text{Tb}_3\text{N}@D_2(35)\text{-C}_{88}$ , 7.245, 8.531, 8.839 Å;  $\text{Tm}_3\text{N}@D_2(35)\text{-C}_{88}$ , 7.273, 8.538, 8.808 Å. Additionally, the dimetallo-endohedral  $\text{Sm}_2@D_2(35)\text{-C}_{88}$  also utilizes the same cage with distances along the twofold axes of 7.241, 8.518, and 8.915 Å and the metal ions situated along the longest axis.<sup>31</sup>

Our results on the structure of  $\text{Gd}_3\text{N}@D_2(35)\text{-C}_{88}$  agree with density functional calculations that indicated that the lowest-energy isomer of  $\text{Gd}_3\text{N}@C_{88}$  would utilize the  $D_2(35)\text{-C}_{88}$  cage.<sup>32</sup> However, similar calculations predict that  $\text{La}_3\text{N}@C_{88}$  will utilize another cage isomer with  $C_s$  symmetry as the most stable structure.<sup>32</sup>

The structure of the  $D_2(35)\text{-C}_{88}$  cage involves 22 different types of carbon atoms as shown in [Figure 4](#). Thus, this is a more complex fullerene cage than the more frequently encountered  $I_h\text{-C}_{80}$  cage, which contains only two types of carbon atoms. The procedures reported here should allow the chemical reactivity of  $\text{Gd}_3\text{N}@D_2(35)\text{-C}_{88}$  to be studied and



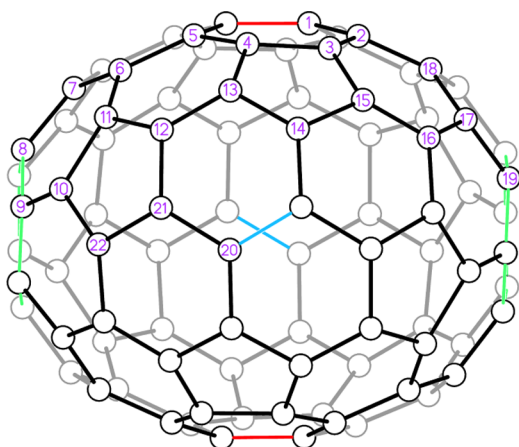


**Figure 4.** Idealized  $D_2(35)\text{-C}_{88}$  cage with the 22 distinct types of carbon atoms individually labeled. The short  $C_2$  axis is aligned vertically and bisects the two red C–C bonds. A second  $C_2$  axis is arranged perpendicular to the plane of the page and bisects the two blue C–C bonds. The third  $C_2$  axis passes through the centers of the two hexagons that are colored green.

compared to that of the relatively inert  $M_3N@I_h\text{-C}_{80}$  family. The  $D_2(35)\text{-C}_{88}$  cage contains all of the bond types that can be found in a cage that obeys the isolated pentagon rule (IPR) including: bonds at a 5:6 ring junction and three types of bonds at 6:6 ring junctions, those with pentagons at either end like the C12–C13 bond (pyracylene sites), those with hexagons at either end like the C5–C6 bond (pyrene sites), and those with a pentagon and a hexagon at either end. In contrast, the  $I_h\text{-C}_{80}$  cage contains C–C bonds at a 5:6 ring junction and only one type of bond at a 6:6 ring junction, a bond with a pentagon and a hexagon at either end like the C15–C16 bond.

Figure 5 shows the orientation of the  $Gd_3N@D_2(35)\text{-C}_{88}$  with respect to the Ni(OEP) molecule. As usual with such cocrystals, the eight ethyl arms of the porphyrin embrace the carbon cage. Inside the cage, the  $Gd_3N$  unit is aligned so that it is almost parallel to the porphyrin plane. The dihedral angle

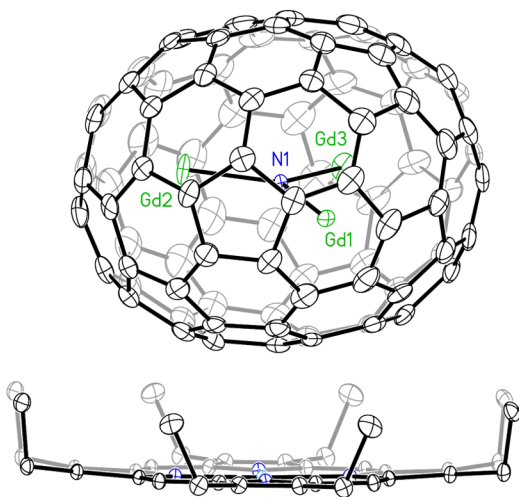


**Figure 5.** Relative positions of one enantiomer of the endohedral fullerene and Ni(OEP) molecule in  $Gd_3N@D_2(35)\text{-C}_{88}\cdot Ni(OEP)\cdot 2(\text{toluene})$ . The color scheme is carbon atoms, black or gray; nitrogen, blue; nickel, turquoise; gadolinium, green. Only the principle orientation of the  $Gd_3N$  unit is shown. The positions of hydrogen atoms and toluene molecules are omitted for clarity.

between the plane of the  $NiN_4$  unit and the  $Gd_3N$  unit is  $17.55^\circ$  for the major orientation of the latter and  $16.97^\circ$  and  $17.68^\circ$  for the other two  $Gd_3N$  orientations. For  $Tb_3N@D_2(35)\text{-C}_{88}\cdot Ni(OEP)\cdot 2.5(\text{benzene})$  and  $Tm_3N@D_2(35)\text{-C}_{88}\cdot Ni(OEP)\cdot 2.5(\text{benzene})$ , the  $M_3N$  units are more tipped with regard to the porphyrin plane. In  $Tb_3N@C_{88}\cdot Ni(OEP)\cdot 2.5(\text{benzene})$ , the dihedral angles between the  $Tb_3N$  and  $NiN_4$  planes are  $40.45^\circ$  and  $42.14^\circ$  for the two orientations present, while in  $Tm_3N@C_{88}\cdot Ni(OEP)\cdot 2.5(\text{benzene})$  the corresponding angles are similar:  $40.14^\circ$  and  $43.26^\circ$ . In contrast, in cocrystals of  $M_3N@I_h\text{-C}_{80}$  with Ni(OEP), the  $M_3N$  unit invariably is aligned perpendicular to the  $NiN_4$  plane with two of the metal ions lying near the nitrogen atoms of the porphyrin as seen in Figure 6.<sup>33–36</sup> In this figure we utilize the structure of  $Tm_3N@I_h\text{-C}_{80}$  rather than  $Gd_3N@I_h\text{-C}_{80}$  because the latter involves an unusual, pyramidalized  $Gd_3N$  unit.<sup>18b</sup> Our results show that the shape of the carbon cage influences the positioning of the  $M_3N$  unit relative to the porphyrin.

## CONCLUSIONS

In summary, a non-chromatographic method of purification of  $Gd_3N@D_2(35)\text{-C}_{88}$  has been developed that uses successive precipitation with  $CaCl_2$  and  $ZnCl_2$  to selectively remove endohedrals from solution and treatment with amino-functionalized silica to remove remaining endohedral fullerenes and empty cage fullerenes. The structure of  $Gd_3N@D_2(35)\text{-C}_{88}$  shows that the planar  $Gd_3N$  unit fits within a somewhat squashed cage.

## EXPERIMENTAL SECTION

**Stage 1: Enrichment of  $Gd_3N@C_{88}$  from Soot Extract by Selective Reaction with Lewis Acids.** *Round 1.* The synthesis of Gd-containing endohedrals utilized graphite rods doped with  $Gd_2O_3$  and copper metal, which were vaporized in an electric-arc generator under a helium/dinitrogen atmosphere to produce fullerene-containing soot.<sup>26</sup> The soot was extracted with carbon disulfide, and the resulting solution was filtered and evaporated to dryness. A 1.5 g portion of this solid extract was dissolved in 1 L of carbon disulfide. The solution was filtered over a  $1\ \mu\text{m}$  polytetrafluoroethylene filter membrane to remove traces of insoluble material.

For Round 1 of the separation scheme, this carbon disulfide solution was poured into a 2 L flask and stirred after the addition of 1.2 g of anhydrous  $CaCl_2$  powder. After 3.75 h, the reaction mixture was filtered with a Buchner funnel to obtain a filter cake. This precipitate was then transferred to a beaker containing 250 g of ice, 250 mL of water, and 500 mL of carbon disulfide for recovery of the endohedrals. After multiple washes with 500 mL of water in a separatory funnel, the decomplexed metallofullerenes were recovered from the bottom layer of carbon disulfide.

*Round 2.* The filtrate from Round 1, which contained unreacted fullerenes and metallofullerenes, was poured into a 2 L round-bottom flask. A portion of 3.4 g of anhydrous  $CaCl_2$  was added, and the reaction was stirred for 7.75 d. The solution was filtered. The filtrate from this reaction mixture was saved for the Round 3 separation. Decomplexation and recovery of precipitated fullerenes and endohedral fullerenes from this Round 2 precipitate was performed as described above.

*Round 3.* The filtrate from Round 2 was transferred into a 2 L round-bottom flask. While the filtrate was stirred, 2.0 g of anhydrous  $ZnCl_2$  powder was introduced. After 4 h of reaction, the mixture was filtered to provide a filtrate for subsequent reaction in Round 4. Decomplexation and recovery of endohedrals from this Round 3 precipitate was obtained as described above.

*Round 4.* The filtrate from Round 3 was transferred to a 2 L round-bottom flask. Addition of 2.1 g of anhydrous  $ZnCl_2$  powder and stirring for 7 d provided precipitate that was enriched in  $Gd_3N@C_{88}$ .

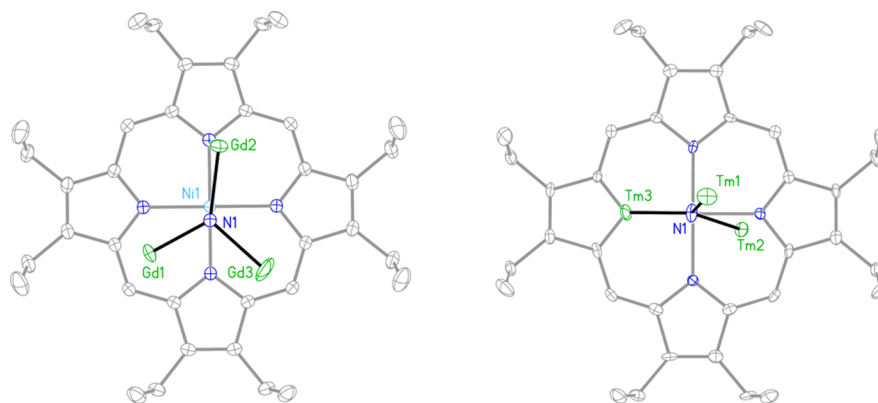


**Figure 6.** Comparison of the orientation of the  $M_3N$  unit relative to the porphyrin in  $Gd_3N@D_2(35)-C_{88}\cdot Ni(OEP)\cdot 2(\text{toluene})$  and in  $Tm_3N@I_h-C_{80}\cdot Ni(OEP)\cdot 2(\text{benzene})$ .<sup>32</sup>

Decomplexation and recovery of endohedrals from this Round 4 precipitate were performed as described above. The filtrate contained empty-cage fullerenes and unreacted endohedrals, which were more chemically resistant to the weak  $CaCl_2$  and  $ZnCl_2$  Lewis acids.

**Stage 2: Isolation of  $Gd_3N@C_{88}$  by Selective Reaction with Aminosilica Gel (SAFA method).** The dried sample of enriched  $Gd_3N@C_{88}$  (i.e., 5 mg of recovered endohedrals from the Round 4 precipitate) was dissolved in 90 mL of freshly purchased xylenes. To this solution was added 4.5 g of monoaminosilica gel, which was prepared as described previously,<sup>12</sup> heated, and vacuum-dried overnight at 60 °C and cooled to ambient temperature under inert gas prior to its addition to the reaction flask. After 22 h of being stirred, the reaction slurry was filtered through a Buchner funnel to provide a filtrate, which contained the isolated  $Gd_3N@C_{88}$ . Note the contaminant endohedrals were immobilized onto the amino-functionalized silica gel. Solvent removal and washing the dried sample with diethyl ether produced 3 mg of an isolated  $Gd_3N@C_{88}$  sample with ~90% purity. A sample of higher purity for X-ray analysis (~99%) was readily obtained by a single pass of HPLC with a BuckyPrep-M column and xylenes as the eluant.

**HPLC Monitoring of Reaction Mixtures.** Aliquots from reaction mixtures of aminosilica were analyzed by HPLC to determine when to stop the SAFA reaction. Chromatographic conditions were as follows: 4.6 mm  $\times$  250 mm BuckyPrep-M stationary phase, 360 nm detection, and 1 mL/min of xylenes.

**LDI Mass Spectrometry.** A Bruker Microflex LT mass spectrometer was used to characterize endohedral samples obtained from Lewis acid and SAFA experiments. The analysis was performed by spotting endohedral samples that were dissolved in  $CS_2$  directly onto the stainless steel target. For each sample well, 1–5  $\mu L$  of fullerene solution was spotted, and no matrix was used. Data were collected in the positive ion mode.

**Structure Determination of  $Gd_3N@D_2(35)-C_{88}\cdot Ni(OEP)\cdot 2C_7H_8$ .** Black blocks were grown by slow diffusion of a toluene solution of  $Gd_3N@C_{88}$  layered over a toluene solution of  $Ni(OEP)$ . Crystal data for  $Gd_3N@D_2(35)-C_{88}\cdot Ni(OEP)\cdot 2$  toluene.  $C_{88}Gd_3N\cdot C_{36}H_{44}N_4Ni\cdot 2(C_7H_8)$ :  $M = 2318.37$ , black parallelepiped,  $\lambda = 0.7449$  Å, Advanced Light Source, beamline 11.3.1, monoclinic, space group  $C2/m$ ,  $a = 25.2389(16)$ ,  $b = 15.3624(9)$ ,  $c = 20.5877(12)$  Å,  $\beta = 94.599(3)^\circ$ ,  $T = 100(2)$  K,  $V = 7956.8(8)$  Å<sup>3</sup>,  $Z = 4$ , 89 654 reflections measured, 19 828 unique ( $R_{int} = 0.053$ ), which were used in all calculations, Bruker SMART Apex II;  $2\theta_{max} = 80.62^\circ$ ; min/max transmission = 0.819/0.516 (multiscan absorption correction applied); full-matrix least-squares based on  $F^2$  (SHELXL-2014/7);<sup>20</sup> the final  $wR(F_2)$  was 0.2670 (all data), conventional  $R1 = 0.0888$  computed for 19 828 reflections with  $I > 2\sigma(I)$  using 983 parameters with 847 restraints.

The asymmetric unit consists of one-half of a  $Gd_3N@D_2(35)-C_{88}$  molecule, one-half of a  $Ni(OEP)$  molecule, and two half toluene molecules. The  $Gd_3N@D_2(35)-C_{88}$ ,  $Ni(OEP)$ , and one toluene reside on the same crystallographic mirror plane. By virtue of the mirror plane, both enantiomers of the  $D_2$ -symmetric fullerene cage occupy

the same site. The fullerene was modeled with suppressed crystallographic symmetry. The interior  $Gd_3N$  cluster was disordered over four orientations. The  $Ni(OEP)$  molecule was fully ordered. One toluene molecule was modeled with suppressed crystallographic symmetry, and the remaining toluene molecule was disordered over two orientations. More refinement details can be found in the [crystallographic information file \(CIF\)](#).

## ■ ASSOCIATED CONTENT

### 📄 Supporting Information

The Supporting Information is available free of charge on the ACS Publications website at DOI: [10.1021/acs.inorgchem.5b01814](https://doi.org/10.1021/acs.inorgchem.5b01814).

Additional LDI mass spectral data. (PDF)

X-ray crystallographic information for  $Gd_3N@D_2(35)-C_{88}\cdot Ni(OEP)\cdot 2(\text{toluene})$ . (CIF)

## ■ AUTHOR INFORMATION

### Corresponding Authors

\*E-mail: [stevens@ipfw.edu](mailto:stevens@ipfw.edu). Phone: +1 (260) 481 6290.

\*E-mail: [mmolmstead@ucdavis.edu](mailto:mmolmstead@ucdavis.edu). Phone: +1 (530) 752 6668. Fax: +1 (530) 752 8995.

\*E-mail: [albalch@ucdavis.edu](mailto:albalch@ucdavis.edu). Phone: +1 (530) 752 0941. Fax: +1 (530) 752 2820.

### Notes

The authors declare no competing financial interest.

## ■ ACKNOWLEDGMENTS

We thank the National Science Foundation (Grant Nos. CHE-1151668 and CHE-1465173 to S.S. and Grant No. CHE-1305125 to A.L.B. and M.M.O.) for support and the Advanced Light Source, supported by the Director, Office of Science, Office of Basic Energy Sciences, of the U.S. Department of Energy under Contract No. DE-AC02-05CH11231, for beam time and fellowship to K.B.G.

## ■ REFERENCES

- (1) Dorn, H. C.; Rice, G.; Glass, T.; Harich, K.; Cromer, F.; Jordan, M. R.; Craft, J.; Hadju, E.; Bible, R.; Olmstead, M. M.; Maitra, K.; Fisher, A. J.; Balch, A. L.; Stevenson, S. *Nature* **1999**, *401*, 55.
- (2) Olmstead, M. M.; Balch, A. L.; Pinzon, J. R.; Echegoyen, L.; Gibson, H. W.; Dorn, H. C. *Chemistry of Nanocarbons*; Wudl, F., Nagase, S., Akasaka, T., Eds.; Blackwell Publishing Ltd., 2010; p 239.
- (3) Chaur, M. N.; Melin, F.; Ortiz, A. L.; Echegoyen, L. *Angew. Chem., Int. Ed.* **2009**, *48*, 7514.
- (4) Popov, A. A.; Yang, S.-F.; Dunsch, L. *Chem. Rev.* **2013**, *113*, 5989.

- (5) Elliott, B.; Yu, L.; Echegoyen, L. *J. Am. Chem. Soc.* **2005**, *127*, 10885.
- (6) Ceron, M. R.; Li, F. F.; Echegoyen, L. *Chem. - Eur. J.* **2013**, *19*, 7410.
- (7) Angeli, C. D.; Cai, T.; Duchamp, J. C.; Reid, J. E.; Singer, E. S.; Gibson, H. W.; Dorn, H. C. *Chem. Mater.* **2008**, *20*, 4993.
- (8) Ge, Z. X.; Duchamp, J. C.; Cai, T.; Gibson, H. W.; Dorn, H. C. *J. Am. Chem. Soc.* **2005**, *127*, 16292.
- (9) Stevenson, S.; Rottinger, K. A.; Field, J. S. *Dalton Trans.* **2014**, *43*, 7435.
- (10) Stevenson, S.; Mackey, M. A.; Pickens, J. E.; Stuart, M. A.; Confait, B. S.; Phillips, J. P. *Inorg. Chem.* **2009**, *48*, 11685.
- (11) Stevenson, S.; Mackey, M. A.; Coumbe, C. E.; Phillips, J. P.; Elliott, B.; Echegoyen, L. *J. Am. Chem. Soc.* **2007**, *129*, 6072.
- (12) Stevenson, S.; Harich, K.; Yu, H.; Stephen, R. R.; Heaps, D.; Coumbe, C.; Phillips, J. P. *J. Am. Chem. Soc.* **2006**, *128*, 8829.
- (13) Stevenson, S.; Rose, C. B.; Robson, A. A.; Heaps, D. T.; Buchanan, J. P. *Fullerenes, Nanotubes, Carbon Nanostruct.* **2014**, *22*, 182.
- (14) Stevenson, S.; Thompson, H. R.; Arvola, K. D.; Ghiassi, K. B.; Olmstead, M. M.; Balch, A. L. *Chem. - Eur. J.* **2015**, *21*, 10362.
- (15) Stevenson, S.; Rottinger, K. A.; Fahim, M.; Field, J. S.; Martin, B. R.; Arvola, K. D. *Inorg. Chem.* **2014**, *53*, 12939.
- (16) Chaur, M. N.; Melin, F.; Elliott, B.; Athans, A. J.; Walker, K.; Holloway, B. C.; Echegoyen, L. *J. Am. Chem. Soc.* **2007**, *129*, 14826.
- (17) Ghiassi, K. B.; Olmstead, M. M.; Balch, A. L. *Dalton Trans.* **2014**, *43*, 7346.
- (18) (a) Beavers, C. M.; Chaur, M. N.; Olmstead, M. M.; Echegoyen, L.; Balch, A. L. *J. Am. Chem. Soc.* **2009**, *131*, 11519. (b) Stevenson, S.; Phillips, J. P.; Reid, J. E.; Olmstead, M. M.; Rath, S. P.; Balch, A. L. *Chem. Commun.* **2004**, 2814. (c) Mercado, B. Q.; Beavers, C. M.; Olmstead, M. M.; Chaur, M. N.; Walker, K.; Holloway, B. C.; Echegoyen, L.; Balch, A. L. *J. Am. Chem. Soc.* **2008**, *130*, 7854. (d) Zuo, T.; Walker, K.; Olmstead, M. M.; Melin, F.; Holloway, B. C.; Echegoyen, L.; Dorn, H. C.; Chaur, M. N.; Chancellor, C. J.; Beavers, C. M.; Balch, A. L.; Athans, A. J. *Chem. Commun.* **2008**, 1067. (e) Chaur, M. N.; Aparicio-Anglés, X.; Mercado, B. Q.; Elliott, B.; Rodríguez-Forteza, A.; Clotet, A.; Olmstead, M. M.; Balch, A. L.; Poblet, J. M.; Echegoyen, L. *J. Phys. Chem. C* **2010**, *114*, 13003.
- (19) Mikawa, M.; Kato, H.; Okumura, M.; Narazaki, M.; Kanazawa, Y.; Miwa, N.; Shinohara, H. *Bioconjugate Chem.* **2001**, *12*, 510.
- (20) Bolskar, R. D.; Benedetto, A. F.; Husebo, L. O.; Price, R. E.; Jackson, E. F.; Wallace, S.; Wilson, L. J.; Alford, J. M. *J. Am. Chem. Soc.* **2003**, *125*, 5471.
- (21) Toth, E.; Bolskar, R. D.; Borel, A.; Gonzalez, G.; Helm, L.; Merbach, A. E.; Sitharaman, B.; Wilson, L. J. *J. Am. Chem. Soc.* **2005**, *127*, 799.
- (22) Shu, C.-Y.; Wang, C.-R.; Zhang, J.-F.; Gibson, H. W.; Dorn, H. C.; Corwin, F. D.; Fatouros, P. P.; Dennis, T. J. *S. Chem. Mater.* **2008**, *20*, 2106.
- (23) Wang, Z. Y.; Nakanishi, Y.; Noda, S.; Akiyama, K.; Shinohara, H. *J. Phys. Chem. C* **2012**, *116*, 25563.
- (24) Akiyama, K.; Hamano, T.; Nakanishi, Y.; Takeuchi, E.; Noda, S.; Wang, Z. Y.; Kubuki, S.; Shinohara, H. *J. Am. Chem. Soc.* **2012**, *134*, 9762.
- (25) Fillmore, H. L.; Shultz, M. D.; Henderson, S. C.; Cooper, P.; Broaddus, W. C.; Chen, Z. J.; Shu, C.-Y.; Zhang, J.-F.; Ge, J. C.; Dorn, H. C.; Corwin, F.; Hirsch, J. I.; Wilson, J.; Fatouros, P. P. *Nanomedicine* **2011**, *6*, 449.
- (26) Chaur, M. N.; Athans, A. J.; Echegoyen, L. *Tetrahedron* **2008**, *64*, 11387.
- (27) Stevenson, S.; Mackey, M. A.; Thompson, M. C.; Coumbe, H. L.; Madasu, P. K.; Coumbe, C. E.; Phillips, J. P. *Chem. Commun.* **2007**, 4263.
- (28) Sarina, E. A.; Mercado, B. Q.; Franco, J. U.; Thompson, C. J.; Easterling, M. L.; Olmstead, M. M.; Balch, A. L. *Chem. Eur. J.* **2015**, *21*, in press. DOI: [10.1002/chem.201502415](https://doi.org/10.1002/chem.201502415)
- (29) Zuo, T.; Beavers, C. M.; Duchamp, J. C.; Campbell, A.; Dorn, H. C.; Olmstead, M. M.; Balch, A. L. *J. Am. Chem. Soc.* **2007**, *129*, 2035.
- (30) Zuo, T.; Dorn, H. C.; Beavers, C. M.; Olmstead, M. M.; Balch, A. L. *Fullerenes, Nanotubes, Carbon Nanostruct.* **2014**, *22*, 280.
- (31) Yang, H.; Jin, H.; Hong, B.; Liu, Z.; Beavers, C. M.; Zhen, H.; Wang, Z.; Mercado, B. Q.; Olmstead, M. M.; Balch, A. L. *J. Am. Chem. Soc.* **2011**, *133*, 16911.
- (32) Xu, L.; Li, S.-F.; Gan, L.-H.; Shu, C.-Y.; Wang, C.-R. *Chem. Phys. Lett.* **2012**, *521*, 81.
- (33) Stevenson, S.; Chancellor, C. J.; Lee, H. M.; Olmstead, M. M.; Balch, A. L. *Inorg. Chem.* **2008**, *47*, 1420.
- (34) Wang, X. L.; Zuo, T. M.; Olmstead, M. M.; Duchamp, J. C.; Glass, T. E.; Cromer, F.; Balch, A. L.; Dorn, H. C. *J. Am. Chem. Soc.* **2006**, *128*, 8884.
- (35) Stevenson, S.; Rose, C. B.; Maslenikova, J. S.; Villarreal, J. R.; Mackey, M. A.; Mercado, B. Q.; Chen, K.; Olmstead, M. M.; Balch, A. L. *Inorg. Chem.* **2012**, *51*, 13096.
- (36) Zuo, T.; Olmstead, M. M.; Beavers, C. M.; Balch, A. L.; Wang, G.; Yee, G. T.; Shu, C.; Xu, L.; Elliott, B.; Echegoyen, L.; Duchamp, J. C.; Dorn, H. C. *Inorg. Chem.* **2008**, *47*, 5234.